6.2 Numerical Simulations of a Landfalling Cold Front Observed During COAST: Rapid Evolution and Responsible Mechanisms

Brian A. Colle*[1], Bradley F. Smull[2], and Ming-Jen Yang[3]
[1]Institute for Terrestrial and Planetary Atmospheres, SUNY- Stony Brook, NY
[2] NOAA/NSSL, Boulder, CO and Dept. of Atmospheric Sciences, Univ. of Washington, Seattle, WA
[3]Dept. of Atmospheric Sciences, Chinese Culture Univ., Taipei, Taiwan

1. INTRODUCTION

One of the major objectives of the Coastal Observation And Simulation with Topography (COAST) field program was to study how landfalling fronts and cyclones are modified by the orography of the U.S. West coast (Bond et al. 1997). This paper is a continuation of the Yu and Smull (2000) study (denoted YS in the remainder of the paper), which used conventional synoptic observations as well as profiler, ground-based and NOAA P-3 airborne Doppler radars to describe the mesoscale structure and evolution of a landfalling frontal system along the northern California coast on 1 December 1995. The study area for this event focussed on a section of coastline characterized by a steep rise of terrain to > 1600 m MSL within 120 km of the shore, which favors the development of terrain-enhanced winds ("barrier jets") and heavy rainfall over the coastal zone.

Two principal findings of YS include: (1) flow blocking by the coastal terrain appeared to enhance the precipitation in the vicinity of the front, including the rapid genesis of a narrow cold-frontal rainband (NCFR) and (2) cumulative radar statistics showed evidence of systematic increase in precipitation towards shore, with mean radar reflectivities within ~40 km of the coast 20-30% larger than those offshore.

Frontal modification near steep topography can result from a wide variety of mechanisms. The most examined terrain effect on a front, which YS addressed, is the role of upstream flow blocking on low-level frontal movement and intensity. However, changes in surface roughness across the coast (Doyle 1997), diabatic processes associated with precipitation (Parker and Thorpe 1995), and changes in the synoptic-scale forcing can also play an important role in frontal evolution even in the absence of terrain. It is difficult to separate these factors which influence frontal evolution using only high resolution observations provided by the COAST experiment. Therefore, this study serves to extend YS's work by conducting a series of high resolution simulations.

2. MM5 SIMULATION OF COAST IOP8

The Penn State/National Center for Atmospheric Research (PSU-NCAR) mesoscale model (MM5 version 2.12) was used in non-hydrostatic mode to simulate this case and to provide additional data for diagnosing the frontal interaction with the coastal mountains. For this simulation, stationary 3 and 9 km domains were nested within a 27 km domain using one-way interfaces. Thirty-two unevenly spaced full-sigma levels were used in the vertical, with the maximum resolution in the boundary layer. Initial atmospheric conditions and sea-surface

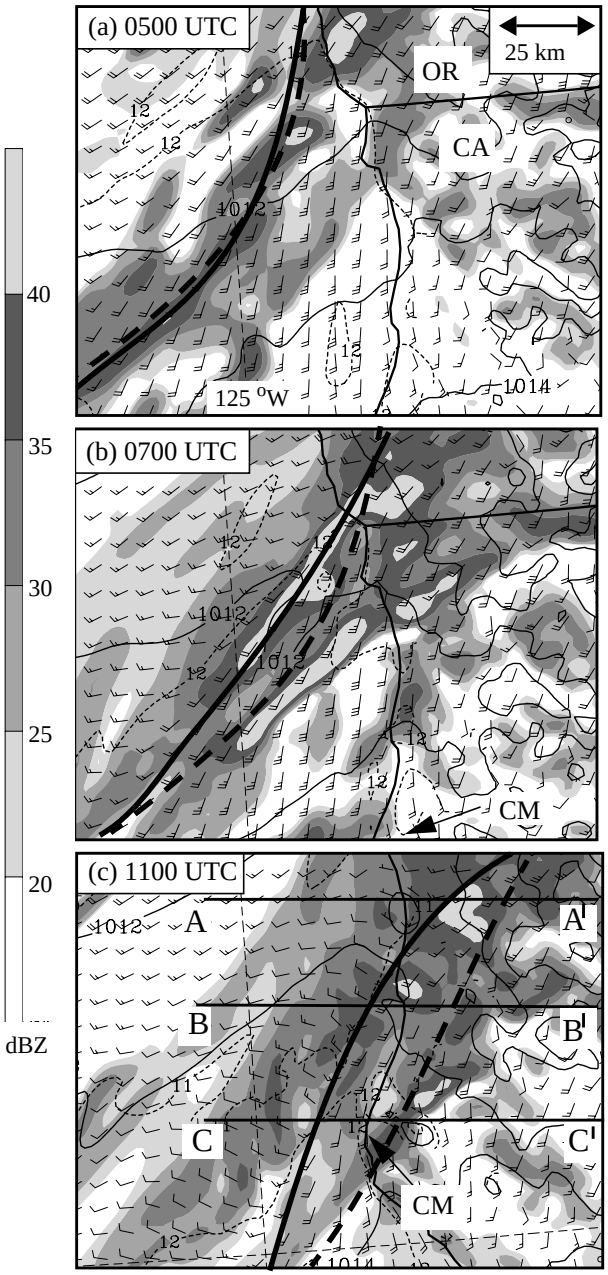

Figure 1. Model surface analysis for a portion of the 3-km domain at (a) 0500 UTC (17 h) and (b) 0700 UTC (19 h), and (c) 1100 UTC (23 h) 1 December 1995 showing sea-level pressure (solid) every 1 mb, winds at 30 m AGL (1 full-barb = 10 kts), and 500-m temperatures (dashed) every 1 °C, and model-derived reflectivities (shaded). The developing surface front is the bold solid line and the 850-mb front is dashed. West-east lines indicate locations for cross sections AA', BB' and CC'.

*Corresponding author address: Dr. Brian A. Colle, Marine Sciences Research Center, University at Stony Brook/SUNY, NY 11794-5000. email: bcolle@notes.cc.sunysb.edu.

temperatures were generated at 1200 UTC 30 November 1995 for the 27, 9, and 3 km domains by first interpolating the National Centers for Environmental Prediction (NCEP) global analyses (2.5^{o} latitude-longitude resolution) to the model grid. These analyses were improved by incorporating surface and upper air observations using a Cressman-type analysis scheme. Four-dimensional data assimilation was applied to the 27-km domain during the first 6 hours of the integration in order to obtain a more realistic simulation. The control (CTL) simulation used the explicit moisture scheme of Reisner et al. (1998), which includes prognostic equations for cloud ice and water, snow, rain, and graupel. The Kain-Fritsch cumulus parameterization (Kain and Fritsch 1990) was applied, except for the inner domain where convective processes could be resolved explicitly. The planetary boundary layer (PBL) was parameterized using the scheme of Zhang and Anthes (1982).

The 3-km simulation illustrates the detailed structure of the front and captures its rapid intensification as it moved southward along the northern California coast (Fig. 1). At 0500 UTC 1 December (Fig. 1a), the developing trough was associated with a 1 ^{o}C temperature drop and confluent flow between ~13 m s^{-1} terrain-parallel southerlies along the coast and ~8 m s^{-1} southwesterlies offshore. Several broken areas of light to moderate precipitation extended from southwest to northeast near this wind transition. By 0700 UTC (Fig. 1b), the frontal precipitation band, temperature gradient, and windshift had intensified, with the southerly prefrontal flow along the northern California coast increasing to 15 m s^{-1} and the surface winds veering from southerly to west-southwesterly across the front. The maximum model reflectivities (> 35 dBZ) and windshift along the front are suggestive of a "classical" NCFR structure confined to a zone within a couple hundred kilometers of the coast. As the front approached Cape Mendocino (CM) by 1100 UTC (cf. Fig. 1c), there was only a broad area of moderate precipitation along the front, and the surface southerlies ahead of the front over the coastal terrain were 5 m s^{-1} weaker than at 0700 UTC. Overall, the MM5 simulation exhibited generally good agreement with the detailed mesoscale field observations regarding the timing, location, and orientation of cold frontal and precipitation evolution, as well as the tendency enhanced precipitation amounts to extend ~25-50 km upwind of the coastal barrier; however, locally the model underestimated the magnitude of the prefrontal barrier jet by as much as 30%.

The northern California coastal topography falls and thus becomes less steep to the south, especially approaching CM; therefore, Fig. 2 shows a series of west-east cross sections to illustrate how the landfalling frontal temperature, wind, and precipitation structures evolved in the presence of this variable terrain. As the front approached the steep coastal topography across section AA' (Fig. 2a), there was a simulated 19 m s^{-1} barrier jet and an intense NCFR near the coast. For section BB' (Fig. 2b), the barrier jet weakened to 15 m s^{-1} and the frontal circulations and associated precipitation began to attenuate. Finally, as the front neared the coast across section CC' (Fig. 2c), the cross-frontal transition in meridional wind weakened with no organized precipitation at the front, and because of shallow low-level terrain blocking the front had developed a more pronounced *forward-tilting* structure with height (also note surface and 850 mb frontal positions on Fig. 1). Overall, these results are consistent with YS, which suggest that the lower coastal topography to the south may have led to the rapid weakening of the frontal circulation and precipitation.

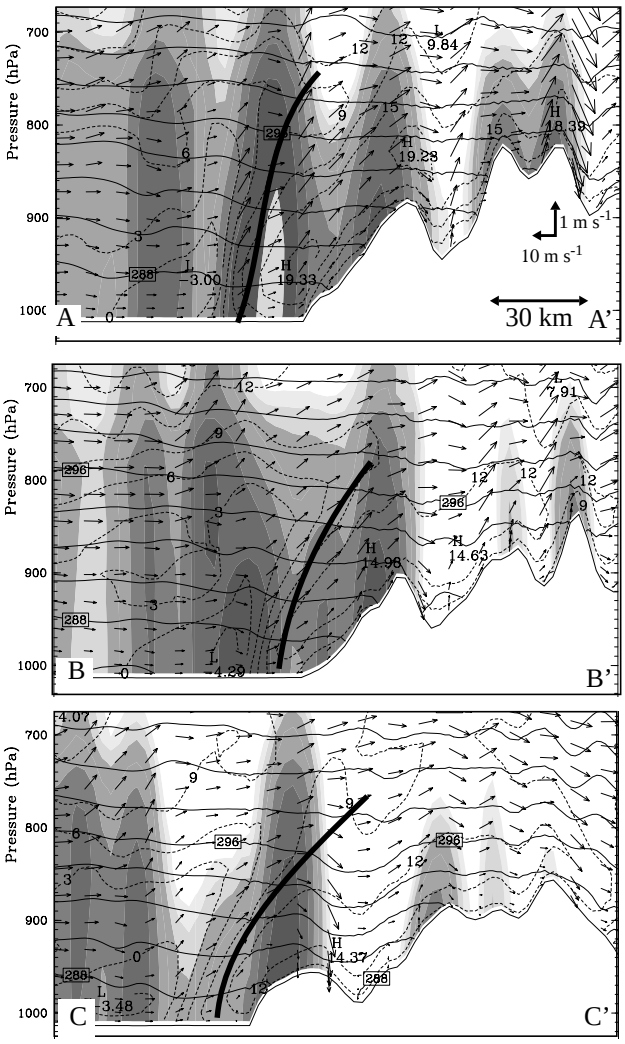

Figure 2: Cross sections (a) AA', (b) BB', and (c) CC' for the 3 km domain at (a) 0900 UTC, (b) 1000 UTC, and (c) 1100 UTC 1 December 1995 showing potential temperature (solid every 1 ^{o}K), model reflectivities (shaded using key in Fig. 1), north-south wind component (dashed every 3 m s^{-1}) and total wind in the cross section. The location of the cross sections are shown in Fig. 1. The front is shown by the solid line.

3. DISCUSSION

An important objective of this study is to determine the mechanism(s) responsible for the rapid intensification of the front and associated precipitation features as they approached the steep coastal topography, as well as the subsequent weakening of the NCFR as the front made landfall further to the south.

The quasi-geostrophic vertical velocity calculated from the MM5 for the 700-500 mb layer was found to increase over the eastern Pacific as the upper-level trough approached the coast (not shown), which suggests that

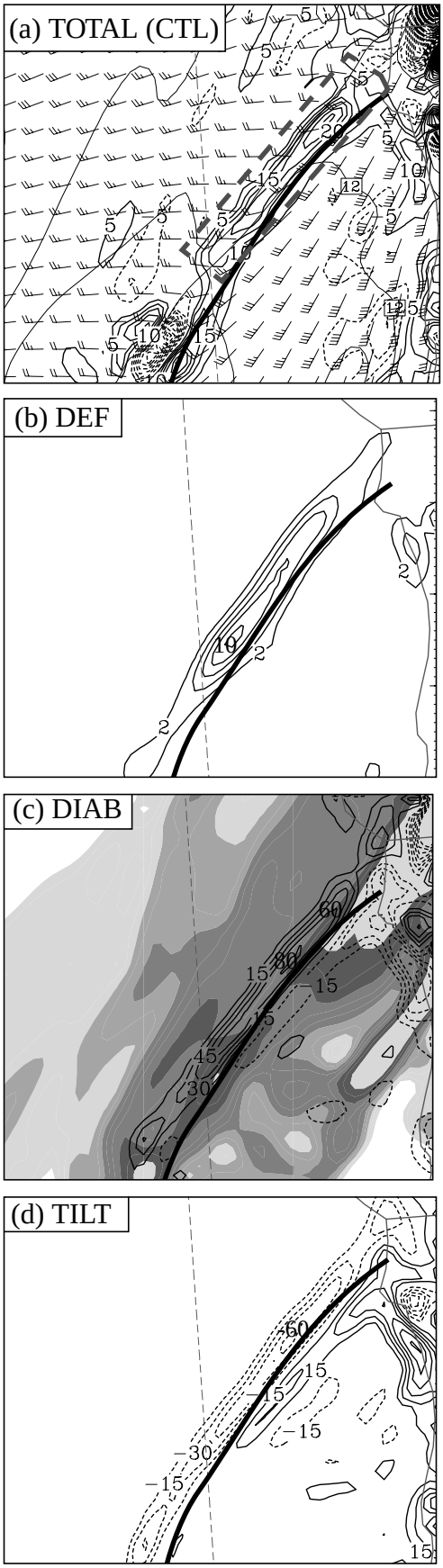

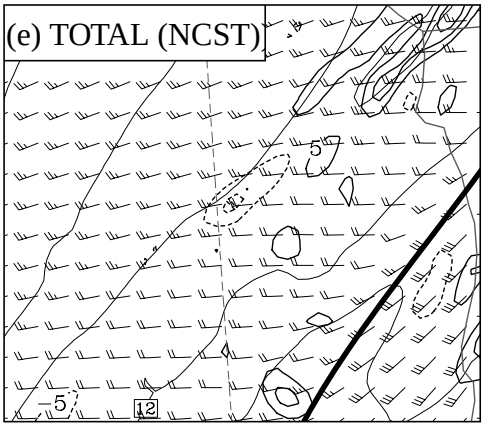

Figure 3. (a) Total, (b) deformation, (c) diabatic, and (d) tilting frontogenesis (thick solid = positive, dashed = negative) for the CTL simulation for 500 MSL at 0800 UTC 1 December (20 h). The total is contoured every 5 ^{o}K (100 km h)$^{-1}$, deformation every 2^{o}K (100 km h)$^{-1}$, and diabatic and tilting every 15 ^{o}K (100 km h)-1. Winds (1 full barb = 10 kts) and 500-m temperatures (thin solid every 0.5 ^{o}C) are shown for reference in (a), and model reflectivities (shaded using scale on Fig. 1) at 500 m are shown in (c). The model frontal position is shown by the bold solid line. (e) Same as (a) except for the NCST simulation. The dashed gray box in (a) is for the frontogenesis traces following the front shown in Fig. 4.

the large-scale forcing was generally favorable for the development of precipitation in the coastal zone between 0300 and 0900 UTC 1 December, albeit on much greater spatial/temporal scales. This result was confirmed by completing a simulation with the topography replaced by flat land within 200 km of the coast (NCST), in which a rapid development of widespread light to moderate coastal precipitation occurred even in the absence of terrain effects (not shown). Obviously, the increased large-scale forcing cannot explain the more intense mesoscale banded nature of precipitation seen in the CTL, therefore the enhanced low-level convergence associated with the barrier jet in the CTL was pivotal in organizing and intensifying the frontal precipitation, particularly within 50 km of the coast. The NCST frontal position along the coast at 0800 UTC 1 December was located at a position near that seen nearly two hours later in the CTL run (Figs. 3a,e), which illustrates that the barrier jet acted to significantly retard the front's forward progression.

The 3-km CTL simulation produced a rapidly developing NCFR along the S. Oregon/ N. California coast. To determine the extent to which this enhancement was associated with an upstream terrain-induced frontogenetical process, the various processes that can act to alter the magnitude of the horizontal potential temperature gradient in a Lagrangian sense were evaluated using Miller's frontogenesis equation (Miller 1948):

$$\frac{d}{dt}\left|\nabla_h\theta\right| = \frac{-1}{\left|\nabla_h\theta\right|}\left\{\underbrace{\left[\left(\frac{\partial\theta}{\partial x}\right)^2\left(\frac{\partial u}{\partial x}\right)+\left(\frac{\partial\theta}{\partial y}\right)^2\left(\frac{\partial v}{\partial y}\right)\right]+\left[\frac{\partial\theta}{\partial x}\frac{\partial\theta}{\partial y}\left(\frac{\partial v}{\partial x}+\frac{\partial u}{\partial y}\right)\right]}_{A}+\right.$$

$$\left.\underbrace{\left[\frac{\partial\theta}{\partial z}\left(\frac{\partial w}{\partial x}\frac{\partial\theta}{\partial x}+\frac{\partial w}{\partial y}\frac{\partial\theta}{\partial y}\right)\right]}_{B}-\underbrace{\left[\frac{\partial\theta}{\partial x}\frac{\partial}{\partial x}\left(\frac{d\theta}{dt}\right)+\frac{\partial\theta}{\partial y}\frac{\partial}{\partial y}\left(\frac{d\theta}{dt}\right)\right]}_{C}\right\} \qquad (1)$$

In (1), the three expressions on the right side are the deformation (A), tilting (B), and diabatic (C) terms, respectively. The diabatic term includes only heating/cooling from precipitation output from the 3-km domain. To assess low-level frontogenesis, the individual terms were calculated at 500 m ASL at 0800 UTC 1 December for the CTL and the NCST simulations (Fig.3).

At 0800 UTC 1 December, the total frontogenesis along the front in the CTL simulation is largest within 100 km of the coast and four times greater than in the NCST run (Fig. 3e). Unlike the NCST simulation, the deformation term made a strong frontogenesis contribution along the frontal zone in CTL, especially near the coast because of enhanced confluence forced by the barrier jet. The differential diabatic effects from precipitation resulted in significant frontogenesis along the front. In contrast, the differential vertical motion at the front results in a negative contribution (frontolysis) by the tilting term immediately west of the front. The diabatic term is greater than the tilting within 50 km of the coast, and dominates the total frontogenesis in this region. There is also net positive frontogenesis in the CTL simulation along the coast to the east of the front associated with the tilting term. This is associated with differential lifting associated with strong upslope flow just inland of the coast (cf. Fig. 2a).

In order to assess further the reasons for the rapid frontal evolution in the coastal zone between 0300 and 1100 UTC 1 December, Fig. 4 shows the frontogenesis terms, average potential temperature gradient at 500 m MSL for a box following the front (cf. Fig. 3a), and the average terrain height to the east of the box from the coast to the edge of the 3-km domain. Between 0300 and 0600 UTC, when the front was offshore and the large-scale forcing was relatively weak, the frontogenesis and low-level convergence contributions were small. As the front approached the coast adjacent to the steep terrain between 0500 and 0800 UTC, the frontogenesis increased rapidly from 3.4 to 9.1 ^{o}K (100 km h)$^{-1}$. During this period the deformation strengthened as a result of increasing convergence between the barrier jet and the front. The enhanced convergence and associated precipitation along the front also resulted in diabatic frontogenesis dominating over the negative contributions from the tilting term. Between 0900 and 1100 UTC as the front sagged south adjacent to lower topography and the barrier jet attenuated (c.f., Fig. 2), the convergence and associated precipitation weakened. As a result, the total frontogenesis was less positive since the negative contributions from the tilting term dominated over diabatics and deformation frontogenesis no longer increased because of weaker convergent flow. Overall, these results support YS's hypothesis that decreased terrain blocking with the lower terrain to the south resulted in an attenuation of the NCFR; however, the frontogenesis results also suggest that diabatics were important in modulating frontal strength near the coast.

The importance of diabatics was also highlighted by conducting an additional simulation in which the latent heating/cooling effects from precipitation were turned off after hour 12 (NOLH). The NOLH run had a significantly weaker frontal temperature gradient near the coast and no banded precipitation (not shown).

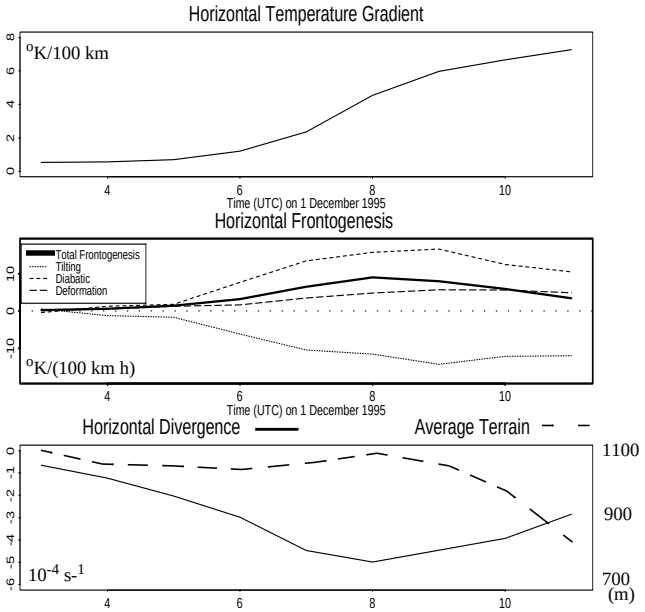

Figure 4. Time series traces at 0.5 km MSL of the potential temperature gradient (^{o}K/100 km), frontogenesis terms (^{o}K/(100 km h), see inset for terms), horizontal divergence (10-4 s^{-1}), and average adjacent coastal terrain (m) for the box shown on Fig. 20a from 0300 to 2300 UTC 1 December 1995.

4. ACKNOWLEDGEMENTS

This research was supported by the Office of Naval Research (Grant No. N00014-00-1-0407 and N00014-97-1-0717). Use of the MM5 was made possible by the Microscale and Mesoscale Meteorological Division of the National Center for Atmospheric Research (NCAR).

5. REFERENCES

Bond, N. A., and co-authors, 1997: The Coastal Observation and Simulation with Topography (COAST) experiment. *Bull. Amer. Meteor. Soc*., **78**, 1941-1955.

Doyle, J. D., 1997: The influence of mesoscale orography on a coastal jet and rainband. *Mon. Wea. Rev.*, **125**, 2152-2175.

Kain, J. S., and J. M. Fritsch, 1990: A one-dimensional entraining/detraining plume model and its application in convective parameterization. *J. Atmos. Sci.*, **47**, 2784-2802.

Miller, J. E., 1948: On the concept of frontogenesis. *J. Meteor.*, **5**, 169-171.

Parker, D. J., and A. J., Thorpe, 1995a: Conditional convective heating in a baroclinic atmosphere: a model of convective frontogenesis. *J. Atmos. Sci.*, **52**, 1699-1711.

Reisner, J., R. M. Rasmussen, and R. T. Bruintjes, 1998: Explicit forecasting of supercooled liquid water in winter storms using the MM5 mesoscale model. *Quart. J. Roy. Meteor. Soc.*, **124**, 1071-1107.

Yu, C-K, and B.F., Smull, 2000: Airborne observations of a landfalling cold front upstream of steep coastal orography. *Mon. Wea. Rev.*, **128**, 1577-1603.

Zhang, D. and R. A. Anthes, 1982: A high-resolution model of the planetary boundary layer-sensitivity test and comparisons with SESAME-79 data. *J. Appl. Meteor.*, **21**, 1594-1609.